Supporting information for

Suppressed Oxidation and Photodarkening of Hybrid Tin Iodide Perovskite Achieved with Reductive Organic Small Molecule

Jue Gong[†#], Xun Li[†#], Wei Huang[§‖], Peijun Guo[‡], Tobin J. Marks[§‖], Richard D. Schaller[§⊥], Tao Xu*[†]

† Department of Chemistry and Biochemistry, Northern Illinois University, DeKalb, IL 60115, United States

‡ Department of Chemical and Environmental Engineering, Yale University, New Haven, CT 06520, United States

§ Department of Chemistry, Northwestern University, 2145 Sheridan Road, Evanston, IL 60208, United States

‖ Materials Research Center, Northwestern University, 2145 Sheridan Road, Evanston, IL 60208, United States

⊥Center for Nanoscale Materials, Argonne National Laboratory, Argonne, IL 60439, United States

# These authors contributed equally.

*Corresponding Author

E-mail: txu@niu.edu (T.X.).

Methods

Chemicals and precursors

Tin(II) iodide (SnI_2, ultra dry, 99.999%) were purchased from Alfa-Aesar. Hydriodic acid (HI, 57% in water), methylamine (CH_3NH_2, 40% in water), dimethyl sulfoxide (DMSO, anhydrous, 99.9+%), dimethylformamide (DMF, anhydrous, 99.8%), and hydroquinone (H_2Q, ≧99%) were purchased from Sigma-Aldrich. Poly(4-Vinylphenol) (PvPh, MW: 22,000) was purchased from Polysciences, Inc. Diethyl ether (anhydrous) and chlorobenzene were purchased from Fisher Chemical. All chemicals and solvents were used as received without further refinement. CH_3NH_3I (MAI) was synthesized by reacting 1: 1.2 molar ratio of HI and CH_3NH_2 in a 100 ml round bottom flask immersed in ice bath and stirred for 2 h. The precipitate was recovered by rotary evaporation at 60 °C to dry off the solvent. The product was washed with diethyl ether several times until it changes to white. Finally, pure MAI product was collected after drying in a vacuum oven at 60 °C overnight.

$MASnI_3$ films preparation

The precursors of $MASnI_3$ and H_2Q:$MASnI_3$ were dissolved in a mixed solvent of DMF and DMSO (2:3 v/v) to form 1 M precursor solutions. In detail, $MASnI_3$ precursor solution was prepared by dissolving 0.186 g SnI_2 and 0.080 g MAI in 0.5 ml of mixed solvent at room

temperature. 0.186 g SnI_2, 0.080 g MAI, and 0.008 g H_2Q were dissolved in 0.5 ml of mixed solvent to form the H_2Q:$MASnI_3$ precursor solution at room temperature. For the preparation of PvPh:$MASnI_3$ precursor solution, 0.2344 g SnI_2, 0.1 g MAI and 0.0046 g PvPh are dissolved in 0.52 mL DMF. Perovskite films were prepared on glass slides which were cleaned by isopropanol, acetone, deionized water, and plasma cleaner in sequence. A spin-coating procedure was executed at 1000 r.p.m for the first 10s, followed by 3000 r.p.m for the second 30s. At 15s before the end of the second spin-coating procedure, 200 μl of chlorobenzene was dropped on the substrate. Subsequently, perovskite films transfer onto a hotplate and annealed at 100 ˚C for 15 min. All the procedures were conducted in an Ar-filled glovebox.

Steady-state and time-resolved photoluminescence (PL)

Tin(II)-based perovskite thin film samples deposited on glass slides were continuously photoexcited with a 700-nm diode laser with 0.5-s exposure time for steady-state PL spectroscopy. For time-resolved PL experiment, emission photons at center wavelengths were collected with a lens and directed to a grating spectrograph with 300-mm focal length as outfitted with a thermoelectrically cooled CCD and avalanche photodiode with time-correlated single-photon counting electronics. TimeHarp 260 software is used to collect the final time-resolved PL decay data with 0.0250 ns per bin.

X-ray Photoelectron Spectroscopy (XPS)

XPS was measured on a Thermo Scientific ESCALAB 250Xi at NUANCE center of Northwestern University, USA. For resolution scans of element photoelectrons, X-ray beam from Al Kα source was applied to form a 900-μm spot after focus. For the mode of photoelectron analyzer, pass energy of 50.0 eV, energy step size of 0.100 eV, 211 energy steps and 31.6 seconds of total acquisition time were used.

Lattice strain calculation

The calculation of material lattice strain follows the Williamson-Hall method, which is based on the broadening of X-ray diffraction peak for indication of strain and size effects, as reported in literatures[1-3]. Specifically, Williamson-Hall plot $\beta_{total} * Cos\theta = \frac{K\lambda}{d} + 4\varepsilon Sin\theta$ describes the crystallite size and strain effects on the diffraction peak full width at half maximum (β_{total}), where θ are Bragg's angles of diffraction peaks, K dimensionless shape factor, λ X-ray wavelength (1.54

Å, Cu Kα radiation in our study), d crystallite size and ε lattice strain of material. As such, the linear fit slope to the $\beta_{total}*Cos\theta$ as a function of $4*Sin\theta$ then represents the strain.

Electrochemical reaction potential of H_2Q

The electrochemical oxidation of H_2Q to quinone (Q) was studied in previous report[4]. When pH is 7.0 of a buffered solution, H_2Q of 1 mM concentration exhibits an oxidation potential of ~0.075 V (vs. saturated calomel electrode (SCE)) at 25±1 °C and scan rate of 100 mV/s. Since standard hydrogen electrode (SHE) potential has relationship $SHE = SCE + 0.241\ V$,[4] we can derive that oxidation of H_2Q to Q as ~0.32 V vs. SHE. It is worthy to mention that in aqueous unbuffered KCl 0.15 M solution, H_2Q of 1 mM concentration shows an oxidation potential of ~0.29 V vs. SCE, or ~0.53 V vs. SHE at 25±1 °C and scan rate of 100 mV/s, which is additionally more spontaneous than the full oxidation of Sn^{2+} to $Sn(OH)_4$ (0.25 V vs. SHE).

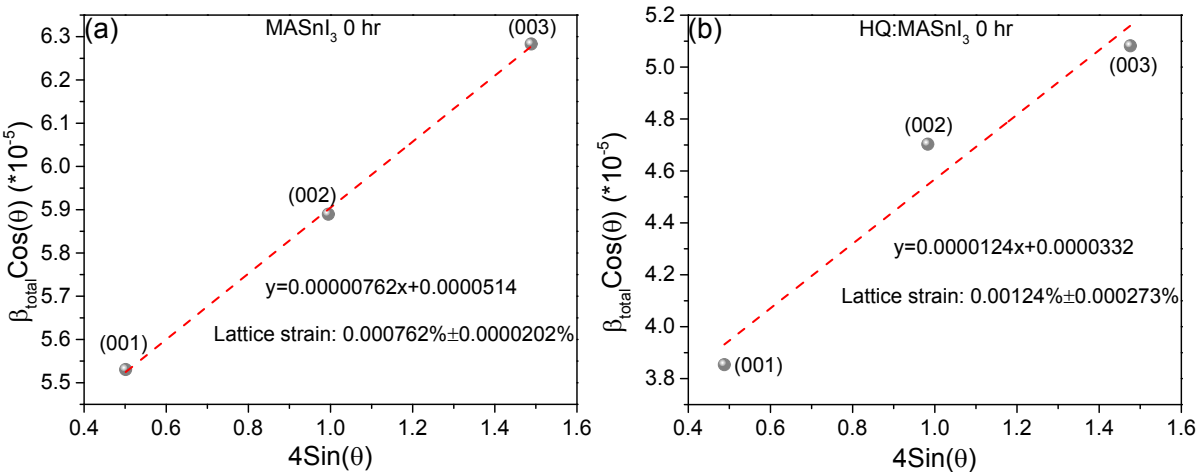

Figure S1. Williamson-Hall plots of as-fabricated pristine $MASnI_3$ (a) and H_2Q-doped $MASnI_3$ (b) films for calculation of their lattice strains.

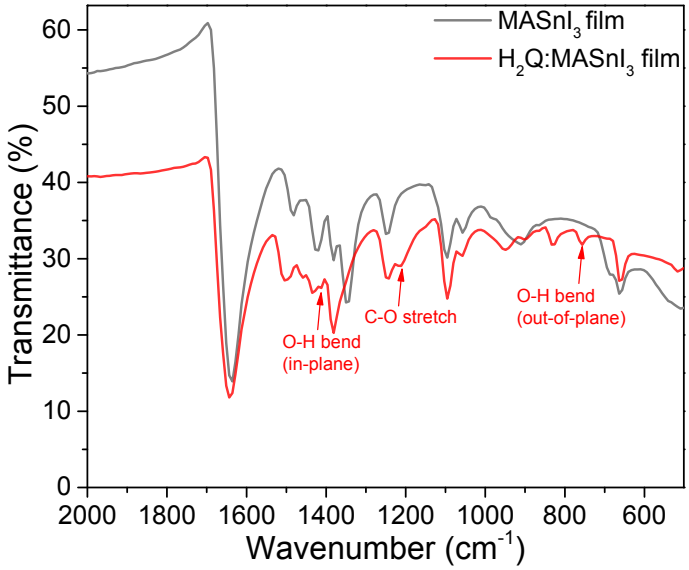

Figure S2. Fourier transform infrared spectra of pristine $MASnI_3$ (gray) and H_2Q:$MASnI_3$ (red) films, where the latter shows vibrational modes belonging to H_2Q and agrees well with previous literature,[5] thus proving the existence of H_2Q in $MASnI_3$.

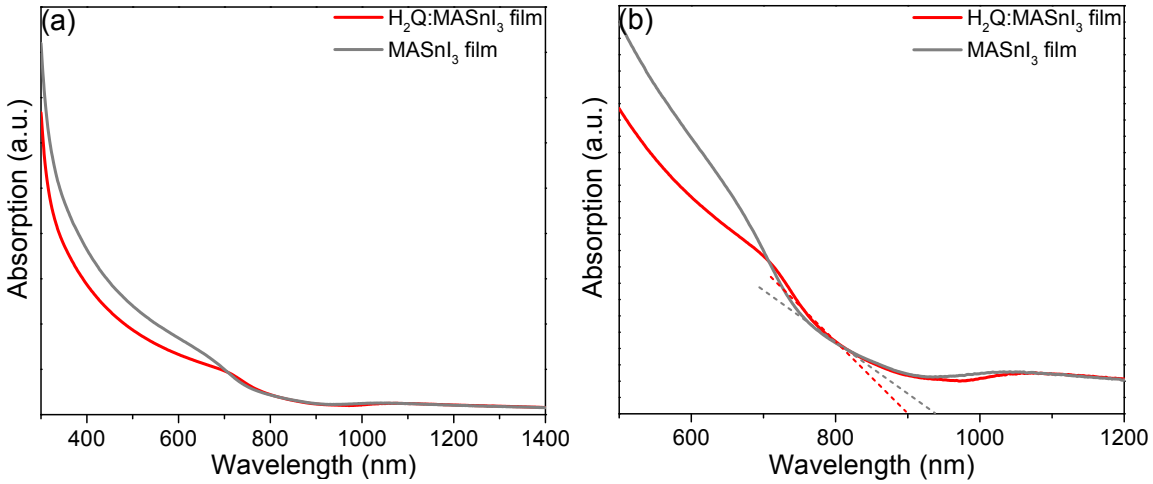

Figure S3. UV-vis absorbance spectra of H_2Q:$MASnI_3$ (red) and pristine $MASnI_3$ (gray) films in (a) full spectral range, (b) close-up view to show the extracted optical bandgaps of 1.38eV and 1.32eV, respectively.

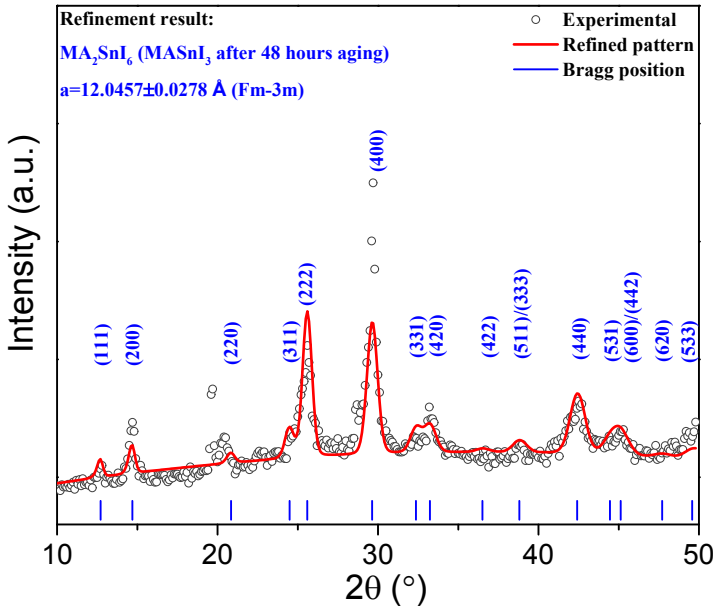

Figure S4. XRD refinement of $MASnI_3$ film after aging in dry air for 48 hours against Cs_2SnI_6 (cubic, Fm-3m)[6] with a refined cell parameter of 12.0457±0.0278 Å, which agrees well with the reported parameter of $(MA)_2SnI_6$,[7] thereby verifying the degradation product as mainly $(MA)_2SnI_6$.

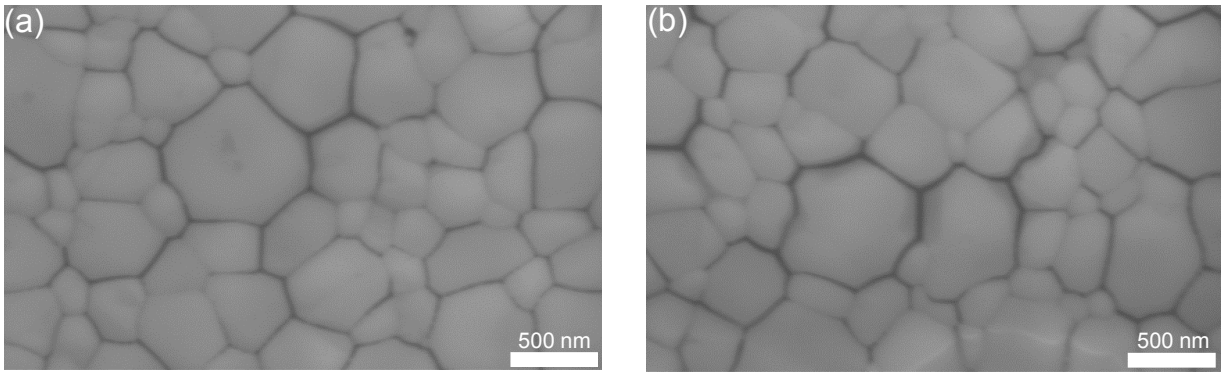

Figure S5. Scanning electron microscopic images of pristine $MASnI_3$ (a) and H_2Q-doped $MASnI_3$ (b) thin films. Both types of perovskite thin films have comparable surface morphology and grain sizes.

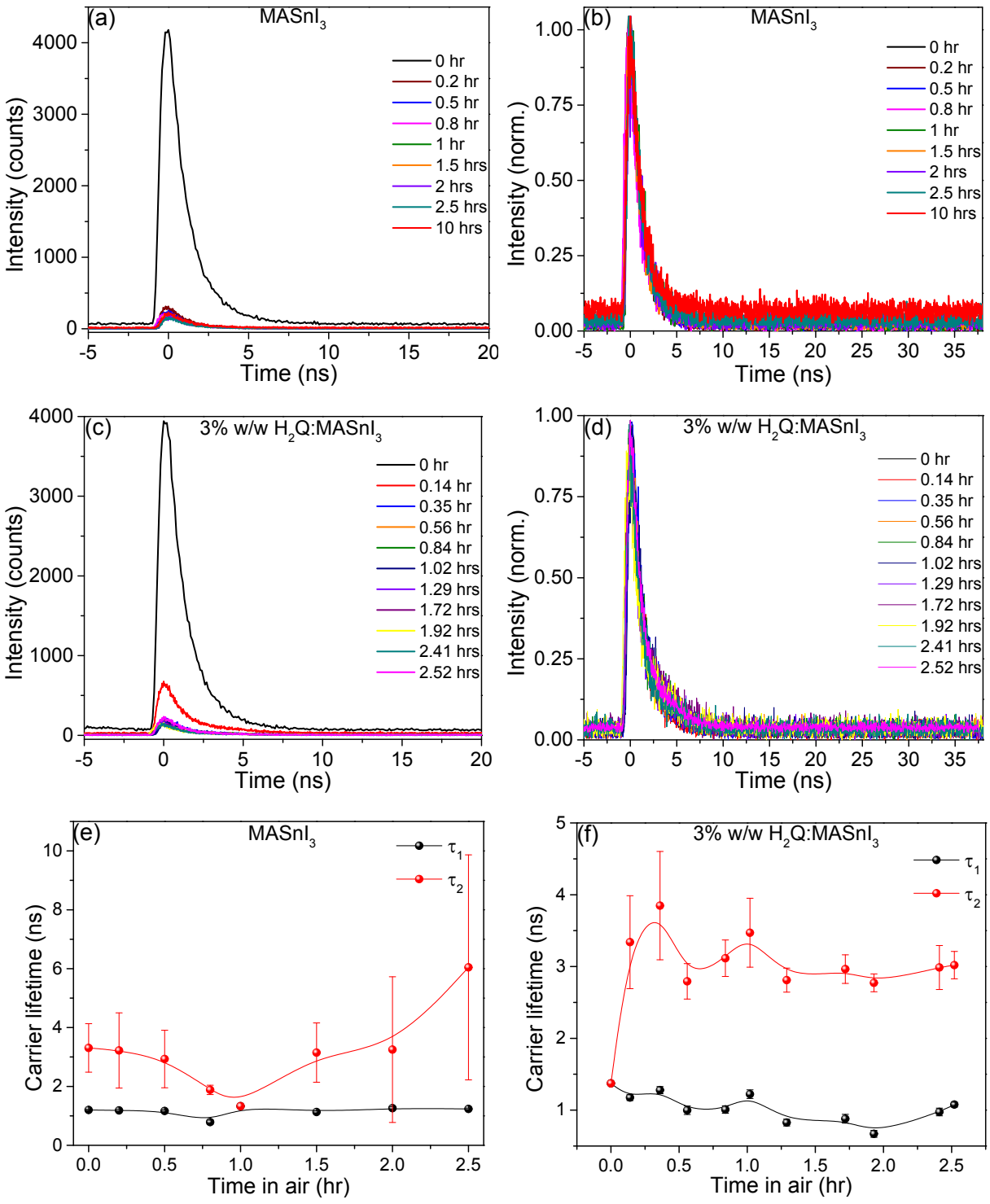

Figure S6. Time-resolved photoluminescence of pristine $MASnI_3$ (a, b) and H_2Q-doped $MASnI_3$ (c, d) films shown in photon counts, normalized scales respectively. (e) and (f) carrier lifetimes as extracted from bi-exponential decay fits for pristine $MASnI_3$ and H_2Q-doped $MASnI_3$ films, respectively.

Table S1. Peak fitting of Sn3d photoelectrons of pristine $MASnI_3$ with 0 hour of exposure to dry air from XPS measurements.

Scan	Start BE (eV)	Peak BE (eV)	End BE (eV)	Area (CPS·eV)	Atomic (%)
Sn3d 5/2 Scan A	499.9	485.516	479.1	452303.19	54.21
Sn3d 3/2 Scan A	499.9	493.916	479.1	313250.52	37.54
Sn3d 5/2 Scan B	499.9	486.562	479.1	40681.52	4.87
Sn3d 3/2 Scan B	499.9	494.962	479.1	28174.69	3.38

Table S2. Peak fitting of Sn3d photoelectrons of pristine $MASnI_3$ with 1 hour of exposure to dry air from XPS measurements.

Scan	Start BE (eV)	Peak BE (eV)	End BE (eV)	Area (CPS·eV)	Atomic (%)
Sn3d 5/2 Scan A	499.9	485.5	479.1	73740.12	3.21
Sn3d 3/2 Scan A	499.9	493.947	479.1	51070.02	2.22
Sn3d 5/2 Scan B	499.9	486.538	479.1	1282823.52	55.87
Sn3d 3/2 Scan B	499.9	494.938	479.1	888427.24	38.70

Table S3. Peak fitting of Sn3d photoelectrons of H_2Q:$MASnI_3$ with 0 hour of exposure to dry air from XPS measurements.

Scan	Start BE (eV)	Peak BE (eV)	End BE (eV)	Area (CPS·eV)	Atomic (%)
Sn3d 5/2 Scan A	499.9	485.312	479.1	433152.64	55.92
Sn3d 3/2 Scan A	499.9	493.712	479.1	299987.47	38.73
Sn3d 5/2 Scan B	499.9	486.501	479.1	24502.19	3.16
Sn3d 3/2 Scan B	499.9	494.901	479.1	16969.41	2.19

Table S4. Peak fitting of Sn3d photoelectrons of H_2Q:$MASnI_3$ with 1 hour of exposure to dry air from XPS measurements.

Scan	Start BE (eV)	Peak BE (eV)	End BE (eV)	Area (CPS·eV)	Atomic (%)
Sn3d 5/2 Scan A	499.9	485.579	479.1	407260.06	33.07
Sn3d 3/2 Scan A	499.9	493.979	479.1	282055.11	22.90
Sn3d 5/2 Scan B	499.9	486.623	479.1	320312.29	26.01
Sn3d 3/2 Scan B	499.9	495.023	479.1	221837.82	18.02

References

(1) Ripolles, T. S.; Yamasuso, D.; Zhang, Y.; Kamarudin, M. A.; Ding, C.; Hirotani, D.; Shen, Q.; Hayase, S. New Tin(II) Fluoride Derivative as a Precursor for Enhancing the Efficiency of Inverted Planar Tin/Lead Perovskite Solar Cells. *J. Phys. Chem. C* **2018**, *122*, 27284-27291.

(2) Zheng, X.; Wu, C.; Jha, S. K.; Li, Z.; Zhu, K.; Priya, S. Improved Phase Stability of Formamidinium Lead Triiodide Perovskite by Strain Relaxation. *ACS Energy Lett.* **2016**, *1*, 1014-1020.

(3) Kumar, D.; Verma, N. K.; Singh, C. B.; Singh, A. K. Crystallite Size Strain Analysis of Nanocrystalline $La_{0.7}Sr_{0.3}MnO_3$ Perovskite by Williamson-Hall Plot Method. *AIP Conf. Proc.* **2018**, *1942*, 050024.

(4) Bard, A. J.; Faulkner, L. R. (2000) Electrochemical Methods: Fundamentals and Applications. John Wiley & Sons, New York.

(5) Kubinyi M. J.; Keresztury G. (1997) Infrared and Raman Spectra of Hydroquinone Crystalline Modifications. In: Mink J., Keresztury G., Kellner R. (eds) Progress in Fourier Transform Spectroscopy. Mikrochimica Acta Supplement, vol 14. Springer, Vienna.

(6) Maughan, A. E.; Ganose, A. M.; Bordelon, M. M.; Miller, E. M.; Scanlon, D. O.; Neilson, J. R. Defect Tolerance to Intolerance in the Vacancy-Ordered Double Perovskite Semiconductors Cs_2SnI_6 and Cs_2TeI_6. *J. Am. Chem. Soc.* **2016**, *138*, 8453-8464.

(7) Funabiki, F.; Toda, Y.; Hosono, H. Optical and Electrical Properties of Perovskite Variant $(CH_3NH_3)_2SnI_6$. *J. Phys. Chem. C* **2018**, *122*, 10749-10754,